International Journal of Microwave and Wireless Technologies

cambridge.org/mrf

Research Paper

Cite this article: Yi Y, Zhu L, Liang L, Fu Y (2023). Reference signal extraction based on multiprocessing method in dual-polarization antenna passive radar. *International Journal of Microwave and Wireless Technologies* **15**, 1154–1164. https://doi.org/10.1017/S1759078722001222

Received: 16 August 2022
Revised: 7 October 2022
Accepted: 10 October 2022

Key words:
Blind adaptive oblique projection; extensive cancellation algorithm; passive radar; polarization diversity; sub-carrier processing

Author for correspondence:
Yucheng Yi, E-mail: ycyi@ecjtu.edu.cn

Reference signal extraction based on multiprocessing method in dual-polarization antenna passive radar

Yucheng Yi[1], Lu Zhu[1], Long Liang[2] and Yan Fu[3]

[1]School of Information Engineering, East China Jiao Tong University, Nanchang, Jiangxi, China; [2]Southwest China Research Institute of Electronic Equipment, Chengdu, Sichuan, China and [3]Wuhan Maritime Communication Research Institute, Wuhan, Hubei, China

Abstract

Extraction of reference signal is an indispensable step in the signal processing of polarization diversity passive radar (PDPR) based on a digital television signal. A conventional reference signal extraction method requires an additional reference antenna, which has a certain demand for space. Single dual-polarization antenna passive radar (SDPPR) systems do not require a reference antenna, and the radar station layout is flexible, which is suitable for a large-scale radar network. It is a main research direction of PDPR in future. However, its reference signal extraction needs to rely on the signal reconstruction method. When the signal to interference and noise ratio of the direct-path signal is relatively low, the signal reconstruction method will fail. In this paper, we propose a reference signal extraction method based on sub-carrier processing method, blind adaptive oblique projection technology, and extensive cancelation algorithm to solve the above problem. Experimental results show that the method proposed in this paper is a reasonable alternative after the failure of reference signal reconstruction, and it is an effective supplement to the reference signal extraction technology.

Introduction

Passive radar or passive coherent location systems have been a hotspot globally [1–7]. Over the decades, illuminators of opportunity used in passive radar have been expanded rapidly, using analog signals such as frequency-modulated commercial radios [2] as well as digital video broadcasting [4], digital audio broadcasting [5], wireless LAN signals [6], global systems for mobile communication signals [7], and china mobile multimedia broadcasting [2] and even LTE signals [8]. With the rapid development of 5G technology [9,10], it will inject vitality into the development of passive radar. One difference between active radar and passive radar is whether the reference signal is extracted. Thus, passive radar systems usually have two types of channels: one is used to receive echo signals of targets called surveillance channel. The other one is used to receive a direct-path signal of illuminators of opportunity called reference channel. The pure reference signal can be used to remove disturbance of the direct-path signal and strong multi-path clutter by time-domain filtering [1] and improve the target signal to noise ratio (SNR) by match filtering [2]. Thus, reference signal extraction is a necessary task in passive radar signal processing flow. The reference signal extraction methods in conventional passive radar based on frequency-modulated signals usually adopt multi-path suppression techniques, such as spatial beam-forming, adaptive filtering in the time domain, and so on [11]. But the signal purity is limited by antenna directivity and the correlation between clutters and direct-path signal. According to passive radar based on digital television signals, the authors in [12–16] propose the reference signal reconstruction (RSR) method. The basic signal reconstruction process is shown in Fig. 1.

The application of conventional passive radars may be challenged by the attributes of the receiving antenna system in terms of size, weight, and cost. In order to reduce the strength of the direct-path signal in the surveillance channel, the angle of the reference antenna and the surveillance antenna need to be separated. This will increase the space requirement of the antenna system, and makes it impossible to setup a passive radar system on certain space-constrained platforms. Meanwhile, cost control is extremely important to realize the large-scale network of passive radar. A single-antenna digital television-based passive radar (SDPR) system can effectively solve the above problems [17]. In order to further improve the anti-jamming capability of the radar system, we propose a single-antenna scheme of the polarization diversity passive radar [18, 19] system on the basis of a slight increase in the cost. Different from the conventional passive radar mode that extract the reference signal from reference channel, the SDPR or the single dual-polarization antenna passive radar (SDPPR) extracts reference signal from the surveillance channel. Fortunately, the RSR method

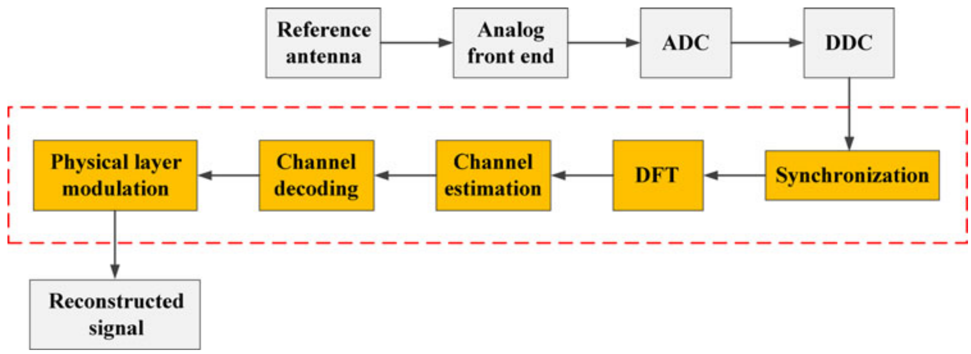

Fig. 1. Signal reconstruction process in passive radar.

is also applicable to the surveillance channel of passive radar, and the signal can be completely recovered under certain signal to interference and noise ratio (SINR) of the direct-path signal conditions (the signal refers to direct-path signal, the interference include multi-path clutter and target signal). However, due to the complex propagation environment and antenna side-lobe attenuation, sometimes SINR of direct-path signal is not ideal in the surveillance channel. The decrease in the SINR of direct-path signal will reduce the purity of reconstructed signal, and even make the signal unable to be reconstructed. This will bring challenges to the RSR method. Assuming that the RSR in surveillance channel cannot be completed, SDPPR system will fail.

In this paper, a new method based on the orthogonal frequency division multiplex (OFDM) modulation of the digital television signal [3], blind adaptive oblique projection technology [20–24], and extensive cancelation algorithm (ECA) [2] is explored to address this difficulty. It is interesting to note that the inter-carrier orthogonality in a multi-path environment means that the zero-Doppler signals are coherent with each other in each sub-carrier. The coherence feature indicates that the direct-path signal and multi-path clutter only occupy one degree of freedom in sub-carrier domain. This feature indicates that the polarization state of composite clutter signal is coherently combined in each sub-carrier. As an effective signal separation method, the largest difference between blind adaptive oblique projection technology and conventional oblique projection in polarization signal processing is that it does not need to obtain the target signal polarization state. It is possible to construct an oblique projection operator only by the composite clutter signal polarization state and achieve signal separation. In order to obtain a more pure reference signal, we use the ECA to filtering the extra multi-path clutter signals and leaving the direct-path signal only. The experimental result shows that the proposed method can extract the reference signal effectively and obtain well target detection effect.

The paper is organized as follows. Section "Signal model" addresses the signal model of SDPPR in the surveillance channel. Section "Theoretical basis" describes the principle of sub-carrier processing, oblique projection, and ECA. Section "Multi-processing method of reference signal extraction" proposes the multi-processing method of the reference signal extraction. In Section "Error analysis," the simulation analyses prove that the method of reference signal extraction-based multi-processing is effective. Section "Experimental research" shows the comparative experimental results. Section "Conclusion" draws conclusions based on the experimental results.

Signal model

SDPPR is a single-antenna passive radar system with polarization diversity capability. The received signal of SDPPR contains direct-path signal, strong clutter, and target echoes.

In this paper, scalars are represented by italic letters, and vectors are represented by bold letters. Suppose the received signal noise is white Gaussian noise. The signal model of SDPPR can expressed in the Jones vector form:

$$\begin{aligned} \boldsymbol{S}_J = \begin{bmatrix} E_H \\ E_V \end{bmatrix} = \begin{bmatrix} E_{dh} \\ E_{dv} \end{bmatrix} c_1 d(t) + \sum_{n=2}^{M_c} \begin{bmatrix} E_{nh} \\ E_{nv} \end{bmatrix} c_n d(t-\tau_n) \\ + \sum_{m=1}^{M_t} \begin{bmatrix} E_{mh} \\ E_{mv} \end{bmatrix} \alpha_m d(t-\tau_m) e^{j2\pi f_m^D t_m} + \begin{bmatrix} w_h \\ w_v \end{bmatrix} \end{aligned} \tag{1}$$

where $d(t)$ is the signal from transmitter. E_{dh}, E_{nh}, and E_{mh} represent direct-path signal, clutters, and targets in the horizontal (H) polarization component, respectively. E_{dv}, E_{nv}, and E_{mv} represent direct-path signal, clutters, and targets in the vertical (V) polarization component, respectively. w_h and w_v represent the Gaussian white noise in the H-polarized channel and V-polarized channel, respectively. c_1, c_n, and α_m represent the amplitude of direct-path signal, clutters, and targets, respectively. τ_n and τ_m represent the delay with respect to the direct-path signal. f_m^D represents the Doppler frequency of the m-th target. M_c and M_t represent the number of clutter and target, respectively.

Theoretical basis

This section will elaborate on the basic principles of sub-carrier processing, oblique projection technology, and ECA.

Sub-carrier processing

Taking a digital television signal based on cyclic prefix (CP-OFDM) as an example, the received signal in the useful duration at k-th sub-carrier can be expressed as [18]:

$$\begin{aligned} S_k = c_1 Q_k^T + \sum_{n=2}^{M_c} c_n e^{-j2\pi f_k \tau_n^c} Q_k^T \\ + \sum_{m=1}^{M_t} \alpha_m e^{-j2\pi (f_k - f_m^D)\tau_m^t} U_{k,m}^T + W_k \end{aligned} \tag{2}$$

https://doi.org/10.1017/S1759078722001222 Published online by Cambridge University Press

where $Q_k = [C_0, k, C_1, k, \ldots, C_{L-1}, k]^T$, L is the OFDM block number used as snapshots, $C_{1,k}$ represent the normalized modulation code of the l-th OFDM block in k-th subcarrier, and

$$U_{k,l} \approx [C_{0,k}, C_{1,k}e^{j2\pi f_l^D T_s}, \ldots, C_{L-1,k}e^{j2\pi f_l^D T_s(L-1)}]^T \quad (3)$$

where T_S is the duration of one OFDM block. It can be seen from (2) that the samples of the direct-path signal and multi-path clutters at one sub-carrier are coherent with each other, whereas target echoes are uncorrelated to the clutter signals due to phase rotation introduced by the Doppler frequency. Therefore, all the zero-Doppler signals as shown in the first term of the right-hand side of (4) are integrated into a single term:

$$\begin{aligned} S_k = &\left[c_1 + \sum_{n=2}^{M_c} c_n e^{-j2\pi f_k \tau_n^c}\right] Q_k^T \\ &+ \sum_{m=1}^{M_t} \alpha_m e^{-j2\pi(f_k - f_m^D)\tau_m^t} U_{k,m}^T + W_k \end{aligned} \quad (4)$$

Oblique projection

Oblique projection operator is an extension of the orthogonal projection operators, which has attracted much attention in the field of signal processing [20]. Oblique projection technology has been used to interference and clutter suppression [25, 26], direction of arrival estimation [21, 27], target detection [28], and polarization diversity technology [22, 24, 29]. Assume that S is a complex matrix of size $n \times m$ having full column rank and, likewise, that J is a complex matrix of size $n \times k$ having full column rank. Assume further that subspace $\langle S \rangle$ and $\langle J \rangle$ are disjoint, which requires $m + k \leq n$. The H represents conjugate transpose symbols. The well-known formula to build a projection with subspace $\langle S \rangle$ is

$$\mathbf{P}_S = \mathbf{S}(\mathbf{S}^H\mathbf{S})^{-1}\mathbf{S}^H \quad (5)$$

where $(\bullet)^H$ represents conjugate transposition. $(\bullet)^{-1}$ represents inverse operation. The orthogonal projection with subspace $\langle S \rangle^\perp$ is given by

$$\mathbf{P}_S^\perp = \mathbf{I} - \mathbf{P}_S \quad (6)$$

Now examine the matrix $(S\ J)$ that is composed from the columns of S and of J. Assume that $m + k < n$, and the column rank of $(S\ J)$ is less than n. The orthogonal projection onto the linear subspace $\langle S\ J \rangle$ is

$$\mathbf{P}_{SJ} = \begin{bmatrix} \mathbf{S} & \mathbf{J} \end{bmatrix} \begin{bmatrix} \mathbf{S}^H\mathbf{S} & \mathbf{S}^H\mathbf{J} \\ \mathbf{J}^H\mathbf{S} & \mathbf{J}^H\mathbf{J} \end{bmatrix}^{-1} \begin{bmatrix} \mathbf{S}^H \\ \mathbf{J}^H \end{bmatrix} \quad (7)$$

We may decompose this orthogonal projection as follows:

$$\mathbf{P}_{SJ} = \mathbf{E}_J + \mathbf{E}_S \quad (8)$$

$$\mathbf{E}_J = \begin{bmatrix} \mathbf{S} & 0 \end{bmatrix} \begin{bmatrix} \mathbf{S}^H\mathbf{S} & \mathbf{S}^H\mathbf{J} \\ \mathbf{J}^H\mathbf{S} & \mathbf{J}^H\mathbf{J} \end{bmatrix}^{-1} \begin{bmatrix} \mathbf{S}^H \\ \mathbf{J}^H \end{bmatrix} \quad (9)$$

$$\mathbf{E}_S = \begin{bmatrix} 0 & \mathbf{J} \end{bmatrix} \begin{bmatrix} \mathbf{S}^H\mathbf{S} & \mathbf{S}^H\mathbf{J} \\ \mathbf{J}^H\mathbf{S} & \mathbf{J}^H\mathbf{J} \end{bmatrix}^{-1} \begin{bmatrix} \mathbf{S}^H \\ \mathbf{J}^H \end{bmatrix} \quad (10)$$

Formulas (9) and (10) may be simplified as follows:

$$\mathbf{E}_J = \mathbf{S}(\mathbf{S}^H\mathbf{P}_J^\perp\mathbf{S})^{-1}\mathbf{S}^H\mathbf{P}_J^\perp \quad (11)$$

$$\mathbf{E}_S = \mathbf{J}(\mathbf{J}^H\mathbf{P}_S^\perp\mathbf{J})^{-1}\mathbf{J}^H\mathbf{P}_S^\perp \quad (12)$$

The subspaces $\langle S \rangle$ and $\langle J \rangle$ are disjoint, so

$$\mathbf{E}_J\begin{bmatrix} \mathbf{S} & \mathbf{J} \end{bmatrix} = \begin{bmatrix} \mathbf{S} & 0 \end{bmatrix} \quad (13)$$

$$\mathbf{E}_S\begin{bmatrix} \mathbf{S} & \mathbf{J} \end{bmatrix} = \begin{bmatrix} 0 & \mathbf{J} \end{bmatrix} \quad (14)$$

As shown in (13) and (14), the oblique projection operator E_J and E_S are orthogonal to the subspace $\langle J \rangle$ and $\langle S \rangle$, respectively. The subspace $\langle S \rangle$ and $\langle J \rangle$ are not required to be orthogonal.

Extensive cancelation algorithm

ECA is a clutter suppression algorithm based on interference subspace projection [2]. The algorithm is to project the echo signals of the surveillance channel into the direct-path signal and its time delay spread space to eliminate clutter. Construct a subspace matrix $\mathbf{X}$ consisting of the reference signal as follows:

$$\mathbf{X} = \begin{bmatrix} S_{ref}(1) & S_{ref}(2) & \cdots & S_{ref}(N) \end{bmatrix}^T \quad (15)$$

where $S_{ref}(n)$, $n = 1, 2, \ldots, N$ represent reference signal and $(\bullet)^T$ represents transposition.

The subspace projection method is used to suppress the direct-path signal and multi-path clutter in the surveillance channel. The orthogonal projection matrix can be represented by the subspace matrix $\mathbf{X}$ formed by the reference signal

$$\mathbf{P} = \mathbf{I} - \mathbf{X}(\mathbf{X}^H\mathbf{X})^{-1}\mathbf{X}^H \quad (16)$$

Projecting the echo signal of the surveillance channel to the orthogonal subspace of the reference signal, the residual signal S_{ECA} in the surveillance channel can be expressed as follows:

$$S_{ECA} = [\mathbf{I} - \mathbf{X}(\mathbf{X}^H\mathbf{X})^{-1}\mathbf{X}^H]S_{surv} = \mathbf{P}S_{surv} \quad (17)$$

After the orthogonal projection processing, the direct-path signal and clutter in the surveillance channel are canceled, and the target signal is retained.

Multi-processing method of reference signal extraction

The SDPPR is a special form of bistatic/multistatic radar system. The illuminators cannot be controlled and are given priority to cover urban areas, thus the surveillance signal contain direct-path signal, strong clutter from environment echoes, and target echoes. Affected by the low SINR of direct-path signal in the surveillance channel, the RSR method is likely to fail, and the radar system will not be able to detect target at this time. In this section, we will introduce a multi-processing method of the reference signal extraction.

https://doi.org/10.1017/S1759078722001222 Published online by Cambridge University Press

The ideal reference channel signal model is shown in (18):

$$\mathbf{S}_J^{ref} = \begin{bmatrix} E_{dh}^{ref} \\ E_{dv}^{ref} \end{bmatrix} l_1 d(t) + \begin{bmatrix} w_h^{ref} \\ w_v^{ref} \end{bmatrix} \tag{18}$$

Comparing (1) and (18), we observed that the target and multipath clutter must be suppressed in order to obtain the ideal reference signal in the surveillance channel. A new reference signal extraction method is proposed in two steps.

Target suppression

It is assumed that the surveillance signal only contains direct-path signal, target signal, and Gaussian white noise, and the polarization state vectors of direct-path signal and target signal can be obtained by estimation, and are expressed as follows:

$$\mathbf{D} = \begin{bmatrix} \cos\gamma_d \\ \sin\gamma_d e^{j\varphi_d} \end{bmatrix} \tag{19}$$

$$\mathbf{T} = \begin{bmatrix} \cos\gamma_t \\ \sin\gamma_t e^{j\varphi_t} \end{bmatrix} \tag{20}$$

Using the method of oblique projection in Section "Theoretical basis," the oblique projection operator can be express as

$$\mathbf{E}_{op} = \mathbf{D}(\mathbf{D}^H \mathbf{P}_T^{\perp} \mathbf{D})^{-1} \mathbf{D}^H \mathbf{P}_T^{\perp} \tag{21}$$

$$\mathbf{E}_{op}\begin{bmatrix} \mathbf{D} & \mathbf{T} \end{bmatrix} = \begin{bmatrix} \mathbf{D} & 0 \end{bmatrix} \tag{22}$$

In (22), the target signal is suppressed. But under actual conditions, the energy of target signal is very low, and its polarization state vector is difficult to estimate. In order to solve this problem, blind adaptive oblique projection technology is used for reference [20–24].

We define the surveillance signal covariance matrix as below:

$$\mathbf{R}_{\mathrm{surv}} = \mathbf{R}_{DT} + \sigma^2 \mathrm{I} = \begin{bmatrix} \mathbf{D} & \mathbf{T} \end{bmatrix} \begin{bmatrix} R_D & 0 \\ 0 & R_T \end{bmatrix} \begin{bmatrix} \mathbf{D} & \mathbf{T} \end{bmatrix}^H + \sigma^2 \mathrm{I} \tag{23}$$

where $\mathbf{R}_{\mathrm{surv}} = \mathbf{S}_{surv}\mathbf{S}_{surv}^H$, $\mathbf{S}_{surv} = \mathbf{D}s_D(t) + \mathbf{T}s_T(t) + \mathbf{W}_{surv}$, $s_D(t) = cd(t)$, $d(t)$ is the signal from transmitter, c represents the amplitude of direct-path signal; $s_T(t) = \alpha d(t-\tau)e^{j2\pi f^D t}$, α represents the amplitude of target, τ represents the delay with respect to the direct-path signal, f^D represents the Doppler frequency of the target; $\mathbf{W}_{surv}$ $\left(\mathbf{W}_{surv} = \begin{bmatrix} w_H & w_V \end{bmatrix}\right)$ represents the Gaussian white noise of H-polarized channel and V-polarized channel; $\mathbf{R}_{DT} = [\mathbf{D}s_D(t) + \mathbf{T}s_T(t)][\mathbf{D}s_D(t) + \mathbf{T}s_T(t)]^H$, R_D $(R_D = [s_D(t)][s_D(t)]^H)$ is the eigenvalue of $\mathbf{R}_{DT}$ related to the direct-path signal. R_T $(R_T = [s_T(t)][s_T(t)]^H)$ is the eigenvalue of $\mathbf{R}_{DT}$ related to the target. σ^2 represents noise variance. $\mathbf{I}$ represents the identity matrix.

Then, we use the method proposed in [30, 31] to estimate the noise variance σ^2, and get $\mathbf{R}_{DT}$ as shown below:

$$\mathbf{R}_{DT} = \mathbf{R}_{surv} - \sigma^2 \mathrm{I} = \begin{bmatrix} \mathbf{D} & \mathbf{T} \end{bmatrix} \begin{bmatrix} R_D & 0 \\ 0 & R_T \end{bmatrix} \begin{bmatrix} \mathbf{D} & \mathbf{T} \end{bmatrix}^H \tag{24}$$

According to the principle of blind adaptive oblique projection, the modified oblique projection operator as follows:

$$\mathbf{E}_{b-op} = \mathbf{D}(\mathbf{D}^H \mathbf{R}_{DT}^{+} \mathbf{D})^{-1} \mathbf{D}^H \mathbf{R}_{DT}^{+} \tag{25}$$

The symbol $(\bullet)^+$ represents the pseudo-inverse. We define

$$\mathbf{A} = \begin{bmatrix} \mathbf{D} & \mathbf{T} \end{bmatrix} \tag{26}$$

$$\mathbf{B} = \begin{bmatrix} R_D & 0 \\ 0 & R_T \end{bmatrix} \tag{27}$$

Then, we can obtain the pseudo-inverse of matrix $\mathbf{A}$:

$$\mathbf{A}^{+} = \begin{bmatrix} (\mathbf{D}^H \mathbf{P}_T^{\perp} \mathbf{D})^{-1} \mathbf{D}^H \mathbf{P}_T^{\perp} \\ (\mathbf{T}^H \mathbf{P}_D^{\perp} \mathbf{T})^{-1} \mathbf{T}^H \mathbf{P}_D^{\perp} \end{bmatrix} \tag{28}$$

where $\mathbf{P}_T^{\perp}$ represents the orthogonal projection matrix of $\mathbf{T}$. $\mathbf{P}_D^{\perp}$ represents the orthogonal projection matrix of $\mathbf{D}$. The covariance matrix of surveillance channel signal without noise can be simplified as

$$\mathbf{R}_{DT}^{+} = (\mathbf{A}\mathbf{B}\mathbf{A}^H)^{+} \tag{29}$$

In order to remove the target signal and extract the reference signal, we need

$$\mathbf{E}_{b-op}\begin{bmatrix} \mathbf{D} & \mathbf{T} \end{bmatrix} = \begin{bmatrix} \mathbf{D} & 0 \end{bmatrix} \tag{30}$$

We can plug (28) and (29) into (25), and get

$$\begin{aligned}
\mathbf{E}_{b-op} &= \mathbf{D}(\mathbf{D}^H \mathbf{R}_{DT}^{+} \mathbf{D})^{-1} \mathbf{D}^H (\mathbf{A}\mathbf{B}\mathbf{A}^H)^{+} \\
&= \mathbf{D}(\mathbf{D}^H \mathbf{R}_{DT}^{+} \mathbf{D})^{-1} (\mathbf{A}^{+}\mathbf{D})^H \mathbf{B}^{-1} \mathbf{A}^{+} \\
&= \mathbf{D}(\mathbf{D}^H \mathbf{R}_{DT}^{+} \mathbf{D})^{-1} \begin{bmatrix} (\mathbf{D}^H \mathbf{P}_T^{\perp} \mathbf{D})^{-1} \mathbf{D}^H \mathbf{P}_T^{\perp} \mathbf{D} \\ (\mathbf{T}^H \mathbf{P}_D^{\perp} \mathbf{T})^{-1} \mathbf{T}^H \mathbf{P}_D^{\perp} \mathbf{D} \end{bmatrix}^H \\
&\quad \mathbf{B}^{-1} \begin{bmatrix} (\mathbf{D}^H \mathbf{P}_T^{\perp} \mathbf{D})^{-1} \mathbf{D}^H \mathbf{P}_T^{\perp} \\ (\mathbf{T}^H \mathbf{P}_D^{\perp} \mathbf{T})^{-1} \mathbf{T}^H \mathbf{P}_D^{\perp} \end{bmatrix} \\
&= \mathbf{D}(\mathbf{D}^H \mathbf{R}_{DT}^{+} \mathbf{D})^{-1} \left(\begin{bmatrix} \mathbf{I} \\ 0 \end{bmatrix} \right)^H \mathbf{B}^{-1} \begin{bmatrix} (\mathbf{D}^H \mathbf{P}_T^{\perp} \mathbf{D})^{-1} \mathbf{D}^H \mathbf{P}_T^{\perp} \\ (\mathbf{T}^H \mathbf{P}_D^{\perp} \mathbf{T})^{-1} \mathbf{T}^H \mathbf{P}_D^{\perp} \end{bmatrix}
\end{aligned} \tag{31}$$

Then, combined with (30) and (31), we can obtain

$$\begin{aligned}
\mathbf{E}_{b-op}\mathbf{T} &= \mathbf{D}(\mathbf{D}^H \mathbf{R}_{DT}^{+} \mathbf{D})^{-1} \left(\begin{bmatrix} \mathbf{I} \\ 0 \end{bmatrix} \right)^H \mathbf{B}^{-1} \begin{bmatrix} (\mathbf{D}^H \mathbf{P}_T^{\perp} \mathbf{D})^{-1} \mathbf{D}^H \mathbf{P}_T^{\perp} \mathbf{T} \\ (\mathbf{T}^H \mathbf{P}_D^{\perp} \mathbf{T})^{-1} \mathbf{T}^H \mathbf{P}_D^{\perp} \mathbf{T} \end{bmatrix} \\
&= \mathbf{D}(\mathbf{D}^H \mathbf{R}_{DT}^{+} \mathbf{D})^{-1} \left(\begin{bmatrix} \mathbf{I} \\ 0 \end{bmatrix} \right)^H \mathbf{B}^{-1} \begin{bmatrix} 0 \\ \mathbf{I} \end{bmatrix} \\
&= \mathbf{D}(\mathbf{D}^H \mathbf{R}_{DT}^{+} \mathbf{D})^{-1} \left(\begin{bmatrix} \mathbf{I} \\ 0 \end{bmatrix} \right)^H \begin{bmatrix} (R_D)^{-1} & 0 \\ 0 & (R_T)^{-1} \end{bmatrix} \begin{bmatrix} 0 \\ \mathbf{I} \end{bmatrix} = 0
\end{aligned} \tag{32}$$

As shown in (32), the target signal is completely removed. However, in the actual working process of the SDPPR, it will inevitably be affected by the complex and variable electromagnetic environment. The electromagnetic wave received by the radar will exhibit a partially polarized wave characteristic. As shown in (1), clutter will cause random modulation of amplitude on the direct-path signal [18].

https://doi.org/10.1017/S1759078722001222 Published online by Cambridge University Press

The composite clutter signal that contains both direct-path signal and random scattered clutter signals is regarded as a random amplitude modulation [18, 20]. In the presence of clutter, the reception signal model is shown as below:

$$\begin{aligned}\mathbf{S} =& \begin{bmatrix} \cos\gamma_d \\ \sin\gamma_d e^{j\varphi_d} \end{bmatrix} c_1 d(t) + \sum_{n=2}^{M_C} \begin{bmatrix} \cos\gamma_c^n \\ \sin\gamma_c^n e^{j\varphi_c^n} \end{bmatrix} c_n d(t-\tau_n) \\ &+ \sum_{m=1}^{M_t} \begin{bmatrix} \cos\gamma_t^m \\ \sin\gamma_t^m e^{j\varphi_t^m} \end{bmatrix} \alpha_m d(t-\tau_t) e^{j2\pi f^{D_t}} + \begin{bmatrix} w_h \\ w_v \end{bmatrix}\end{aligned} \tag{33}$$

where γ_d and ϕ_d represent polarization angle and polarization phase difference of the direct-path signal, respectively. γ_c^n and φ_c^n represent polarization angle and polarization phase difference of clutter, respectively. γ_t^m and φ_t^m represent polarization angle and polarization phase difference of target, respectively.

According to (4), we rewrite (33) and get

$$\begin{aligned}\mathbf{S} =& \begin{bmatrix} (1+\beta_h)\cos\gamma_d \\ (1+\beta_v)\sin\gamma_d e^{j\varphi_d} \end{bmatrix} \varepsilon d(t) \\ &+ \sum_{m=1}^{M_t} \begin{bmatrix} \cos\gamma_t^m \\ \sin\gamma_t^m e^{j\varphi_t^m} \end{bmatrix} \alpha_m d(t-\tau_t) e^{j2\pi f^{D_t}} + \begin{bmatrix} w_h \\ w_v \end{bmatrix}\end{aligned} \tag{34}$$

where ϵ represents the amplitude of the composite clutter signal, β_h represents amplitude modulation factor of H-polarized channel. β_v represents channel amplitude modulation factor of V-polarized. β_h and β_v follow normal distribution.

In order to avoid the influence of amplitude modulation in (34), we will use sub-carrier processing technology. Convert (34) into sub-carrier expression

$$\begin{aligned}\mathbf{S}_k =& \begin{bmatrix} c_{1,h} + \sum_{n=2}^{M_c} c_{n,h} e^{-j2\pi f_k \tau_n} \\ c_{1,v} + \sum_{n=2}^{M_c} c_{n,v} e^{-j2\pi f_k \tau_n} \end{bmatrix} Q_k^T \\ &+ \begin{bmatrix} \sum_{m=1}^{M_t} \alpha_{m,h} e^{-j2\pi(f_k - f_m^D)\tau_m} \\ \sum_{m=1}^{M_t} \alpha_{m,v} e^{-j2\pi(f_k - f_m^D)\tau_m} \end{bmatrix} U_{k,m}^T + \begin{bmatrix} W_{k,h} \\ W_{k,v} \end{bmatrix}\end{aligned} \tag{35}$$

where $c_{1,h}$ and $c_{1,v}$ represent the complex amplitude of direct-path signal in the H-polarized channel and V-polarized channel, respectively. $c_{n,h}$ and $c_{n,v}$ represent the complex amplitude of the n-th stationary multi-path clutters in the H-polarized channel and V-polarized channel, respectively. τ_n represents the delay of the n-th stationary multi-path clutters. $\alpha_{m,h}$ and $\alpha_{m,v}$ represent the complex amplitude of target in the H-polarized channel and V-polarized channel, respectively. τ_m and f_m^D are the delay and the Doppler frequency of m-th target, respectively. M_c and M_t represent the number of multi-path clutter and target, respectively. $W_{k,h}$ and $W_{k,v}$ represents white Gaussian noise in the H-polarized channel and V-polarized channel, respectively.

$\left[c_{1,h} + \sum_{n=2}^{M_c} c_{n,h} e^{-j2\pi f_k \tau_n}\right]$ and $\left[c_{1,v} + \sum_{n=2}^{M_c} c_{n,v} e^{-j2\pi f_k \tau_n}\right]$ could be viewed as the composite weight of clutters in the H-polarized and V-polarized channels, and in each sub-carrier the composite weight is constant.

Considering single target, (35) may be simplified as

$$\mathbf{S}_k = \mathbf{D}_k^{cs} \varepsilon_k Q_k^T + \mathbf{T}_k^t \alpha_k e^{-j2\pi(f_k - f^D)\tau^t} U_k^T + \begin{bmatrix} W_{k,h} \\ W_{k,v} \end{bmatrix} \tag{36}$$

$\mathbf{D}_k^{cs} = \begin{bmatrix} \cos\gamma_k^c \\ \sin\gamma_k^c e^{j\varphi_k^c} \end{bmatrix}$ represents polarization vector of composite clutter signal in the k-th sub-carrier. γ_k^c and φ_k^c represent polarization angle and polarization phase difference of composite clutter signal. $\mathbf{T}_k^t = \begin{bmatrix} \cos\gamma_k^t \\ \sin\gamma_k^t e^{j\varphi_k^t} \end{bmatrix}$ represents polarization vector of target in the k-th sub-carrier. γ_k^t and φ_k^trepresent polarization angle and polarization phase difference of target. ε_k and α_k represent the amplitude of the composite clutter signal and target in the k-th sub-carrier.

The blind adaptive oblique projection operator in each sub-carrier can be expressed as follows:

$$\mathbf{E}_k^{b-op} = \mathbf{D}_k^{cs}((\mathbf{D}_k^{cs})^H (\mathbf{R}_k^{DT})^+ \mathbf{D}_k^{cs})^{-1} (\mathbf{D}_k^{cs})^H (\mathbf{R}_k^{DT})^+ \tag{37}$$

$$\mathbf{R}_k^{DT} = (\mathbf{A}_k \mathbf{B}_k \mathbf{A}_k^H)^+ \tag{38}$$

where $\mathbf{A}_k = \begin{bmatrix} \mathbf{D}_k^{DT} & \mathbf{T}_k^t \end{bmatrix}$ and $\mathbf{B}_k = \begin{bmatrix} R_{k,D} & 0 \\ 0 & R_{k,T} \end{bmatrix}$.

Combining (36) and (37), we can effectively suppress the target signal:

$$\begin{aligned}\mathbf{S}_k^{b-op} &= \mathrm{E}_k^{b-op} \mathbf{S}_k = \mathbf{D}_k^{cs}((\mathbf{D}_k^{cs})^H (\mathbf{R}_k^{DT})^+ \mathbf{D}_k^{cs})^{-1} (\mathbf{D}_k^{cs})^H (\mathbf{R}_k^{DT})^+ \mathbf{S}_k \\ &= \mathbf{D}_k^{cs} \varepsilon_k Q_k^T + \begin{bmatrix} \tilde{W}_k^h \\ \tilde{W}_k^v \end{bmatrix}\end{aligned} \tag{39}$$

where $\tilde{W}_k^h = E_k^{b-op} W_k^h$ and $\tilde{W}_k^v = E_k^{b-op} W_k^v$. As shown in (39), the composite clutter signal is extracted and the target signal is suppressed.

Reference signal purification

Performing IDFT on the data obtained in the previous step to convert the frequency domain signal into the time domain. At this point, the target signal has been suppressed, leaving only the composite signal containing the direct-path wave and zero-Doppler multi-path clutter with different time delays. In order to obtain a purer reference signal, we need to further suppress multi-path clutter. Therefore, we will study in detail the use of ECA to suppress multi-path clutter in this section.

Assume that the transmitted signal is V-polarized polarization, the energy of direct-path signal received by the V-polarized channel is much stronger than that of the H-polarized channel in general. Thus, we consider extracting the direct-path signal in the V-polarized channel and construct composite signal delay subspace matrix $\mathbf{C}_v$ as follows:

$$\mathbf{C}_v = \begin{bmatrix} 0 & S_{sc}^v(1) & S_{sc}^v(2) & \cdots & S_{sc}^v(N-1) \\ 0 & 0 & S_{sc}^v(1) & \cdots & S_{sc}^v(N-2) \\ \vdots & \vdots & \vdots & \ddots & \vdots \\ 0 & 0 & 0 & \cdots & S_{sc}^v(N-K+1) \end{bmatrix}^T \tag{40}$$

https://doi.org/10.1017/S1759078722001222 Published online by Cambridge University Press

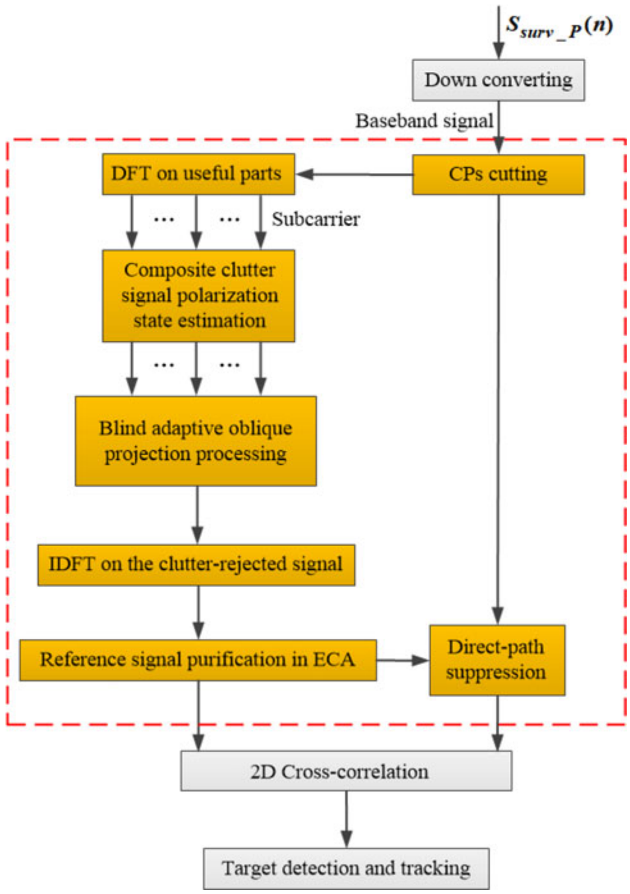

Fig. 2. Signal processing flow of combined processing method.

where $S_{sc}^{v}(n)$ $n = 1, 2, \ldots, N$ represents composite signal in the V-polarized channel. N represents the total data length. K represents the number of cancelation distance cells. In matrix $\mathbf{C}_v$, the first row to the $(K-1)$-th row represent delay of one range bin to $(K-1)$-th range bin in sample signal, respectively.

According to the orthogonal characteristics of the subspace, the orthogonal projection operator can be obtained as

$$\mathbf{P}_{sc}^{v} = \mathbf{I} - \mathbf{C}_v(\mathbf{C}_v^H\mathbf{C}_v)^{-1}\mathbf{C}_v^H \tag{41}$$

The residual signal $S_{ECA,d}^{v}$ in the V-polarized channel of surveillance signal can be expressed as follows:

$$S_{ECA,d}^{v} = [\mathbf{I} - \mathbf{C}_v(\mathbf{C}_v^H\mathbf{C}_v)^{-1}\mathbf{C}_v^H]S_{sc}^{v} = \mathbf{P}_{sc}^{v}S_{sc}^{v} \tag{42}$$

where $S_{ECA,d}^{v}$ is the purified reference signal.

The signal processing flow of SDPPR by using the new method of reference extraction is shown in Fig. 2.

As shown in Fig. 2, the echo signal has been received in the surveillance channel by the single dual-polarization antenna. After the echo signal is processed by sub-carrier, blind adaptive oblique projection technology and ECA, the pure reference signal is obtained. Then, we can suppress the direct-path signal and multipath clutters by employing signal processing method of [32].

Error analysis

It can be seen from (24) and (32), the estimation precision of noise variance σ^2 has an effect on target signal suppression. Assume that there is error in estimation of noise variance in each sub-carrier. Then, matrix $\tilde{\mathbf{B}}_k$ can be expressed as

$$\begin{aligned}\tilde{\mathbf{B}}_k = \begin{bmatrix} R_{k,D} & 0 \\ 0 & R_{k,T} \end{bmatrix} + \begin{bmatrix} \mathbf{D}_k^{cs} & \mathbf{T}_k^t \end{bmatrix}^{-1} \begin{bmatrix} \Delta\sigma^2 & 0 \\ 0 & \Delta\sigma^2 \end{bmatrix} \\ \times \left(\begin{bmatrix} \mathbf{D}_k^{cs} & \mathbf{T}_k^t \end{bmatrix}^H\right)^{-1}\end{aligned} \tag{43}$$

where $\Delta\sigma^2$ represents estimation error of noise variance.

Assume that

$$\begin{bmatrix} \mathbf{D}_k^{cs} & \mathbf{T}_k^t \end{bmatrix}^{-1} = \begin{bmatrix} \kappa_x & \mu_x \\ \kappa_y & \mu_y \end{bmatrix} \tag{44}$$

$$\begin{aligned}\tilde{\mathbf{B}}_k &= \begin{bmatrix} R_{k,D} & 0 \\ 0 & R_{k,T} \end{bmatrix} + \begin{bmatrix} (\kappa_x\kappa_x^*+\mu_x\mu_x^*)\Delta\sigma^2 & (\kappa_x\kappa_y^*+\mu_x\mu_y^*)\Delta\sigma^2 \\ (\kappa_x^*\kappa_y+\mu_x^*\mu_y)\Delta\sigma^2 & (\kappa_y\kappa_y^*+\mu_y\mu_y^*)\Delta\sigma^2 \end{bmatrix} \\ &= \begin{bmatrix} R_{k,D} + (\kappa_x\kappa_x^*+\mu_x\mu_x^*)\Delta\sigma^2 & (\kappa_x\kappa_y^*+\mu_x\mu_y^*)\Delta\sigma^2 \\ (\kappa_x^*\kappa_y+\mu_x^*\mu_y)\Delta\sigma^2 & R_{k,T} + (\kappa_y\kappa_y^*+\mu_y\mu_y^*)\Delta\sigma^2 \end{bmatrix}\end{aligned} \tag{45}$$

It is assumed that the polarization state estimation of composite clutter signal is unbiased estimation. Then, formula (32) can be expressed as

$$\begin{aligned}\mathbf{E}_k^{b-op}\mathbf{T}_k^t &= \mathbf{D}_k^{cs}((\mathbf{D}_k^{cs})^H(\mathbf{A}_k\tilde{\mathbf{B}}_k\mathbf{A}_k^H)^+\mathbf{D}_k^{cs})^{-1}\left(\begin{bmatrix}\mathbf{I}\\0\end{bmatrix}\right)^H \\ &\quad \tilde{\mathbf{B}}_k^{-1}\begin{bmatrix} ((\mathbf{D}_k^{cs})^H\mathbf{P}_T^{\perp}\mathbf{D}_k^{cs})^{-1}(\mathbf{D}_k^{cs})^H\mathbf{P}_T^{\perp} \\ ((\mathbf{T}_k^t)^H\mathbf{P}_D^{\perp}\mathbf{T}_k^t)^{-1}(\mathbf{T}_k^t)^H\mathbf{P}_D^{\perp} \end{bmatrix}\mathbf{T}_k^t \\ &= \mathbf{D}_k^{cs}((\mathbf{D}_k^{cs})^H(\mathbf{A}_k\tilde{\mathbf{B}}_k\mathbf{A}_k^H)^+\mathbf{D}_k^{cs})^{-1}\left(\begin{bmatrix}\mathbf{I}\\0\end{bmatrix}\right)^H\tilde{\mathbf{B}}_k^{-1}\begin{bmatrix}0\\\mathbf{I}\end{bmatrix} \\ &= \mathbf{D}_k^{cs}((\mathbf{D}_k^{cs})^H(\mathbf{A}_k\tilde{\mathbf{B}}_k\mathbf{A}_k^H)^+\mathbf{D}_k^{cs})^{-1}\left(\begin{bmatrix}\mathbf{I}\\0\end{bmatrix}\right)^H \\ &\quad \begin{bmatrix} R_{k,D} + (\kappa_x\kappa_x^*+\mu_x\mu_x^*)\Delta\sigma^2 & (\kappa_x\kappa_y^*+\mu_x\mu_y^*)\Delta\sigma^2 \\ (\kappa_x^*\kappa_y+\mu_x^*\mu_y)\Delta\sigma^2 & R_{k,T} + (\kappa_y\kappa_y^*+\mu_y\mu_y^*)\Delta\sigma^2 \end{bmatrix}\begin{bmatrix}0\\\mathbf{I}\end{bmatrix} \\ &= \mathbf{D}_k^{cs}\frac{(\kappa_x\kappa_y^*+\mu_x\mu_y^*)\Delta\sigma^2}{R_{k,D}+(\kappa_x\kappa_x^*+\mu_x\mu_x^*)\Delta\sigma^2} \\ &= \begin{bmatrix}\cos\gamma_k^c \\ \sin\gamma_k^c\cdot e^{j\varphi_k^c}\end{bmatrix}\frac{-\sin\gamma_k^t\sin\gamma_k^c e^{j(\varphi_k^t-\varphi_k^c)} - \cos\gamma_k^t\cos\gamma_k^c}{MM^*(R_D/\Delta\sigma^2)+1}\end{aligned} \tag{46}$$

where $M = \cos\gamma_k^t\sin\gamma_k^c e^{j\varphi_k^c} - \cos\gamma_k^c\sin\gamma_k^t e^{j\varphi_k^t}$.

The suppression performance of target signal depends on the ratio between the composite clutter signal energy ($R_{k,D}$) and the estimation error of noise variance ($\Delta\sigma^2$) (CENR). The simulation parameters are shown in Table 1.

https://doi.org/10.1017/S1759078722001222 Published online by Cambridge University Press

Table 1. Simulation parameters

	Polarization angle (°)	Phase difference (°)	CENR (dB)
Target	30	0	10:50
Composite clutter signal	75	0	

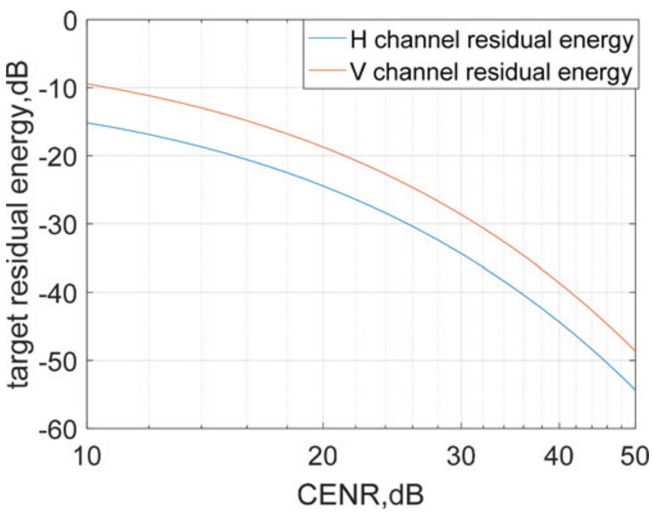

Fig. 3. Relationship between target signal residual energy and CENR.

The relationship between target signal residual energy and CENR is shown in Fig. 3. With the increase of CENR in both *H*-polarized channel and *V*-polarized channel, the target residual energy gradually decreases.

Experimental research

In the flow of signal processing of SDPPR, the extraction of reference signal is an important step. The reference signal can improve the SNR of target in the surveillance channel through matched filtering technology and time-domain clutter suppression method. In this section, we will verify the effectiveness of the proposed method from an experimental perspective.

Experimental scheme

The method proposed in this paper is an effective alternative when the SDPPR system RSR fails. In order to compare the performance of the proposed method, a reference antenna was added on the SDPPR system.

We will obtain the reference signal in two ways. (1) The reference signal is extracted from the reference channel using RSR method. The direct-path signal with high SNR can be obtained by using reference antenna point to the transmitting station. (2) Reference signal extraction in SDPPR based on multi-processing (RSMP) method. When the direct-path signal SNR of SDPPR system surveillance channel is low, the reference signal cannot be reconstructed, and the radar system fails. The combined processing method proposed in this paper can effectively extract the reference signal and restore the working state of the radar system.

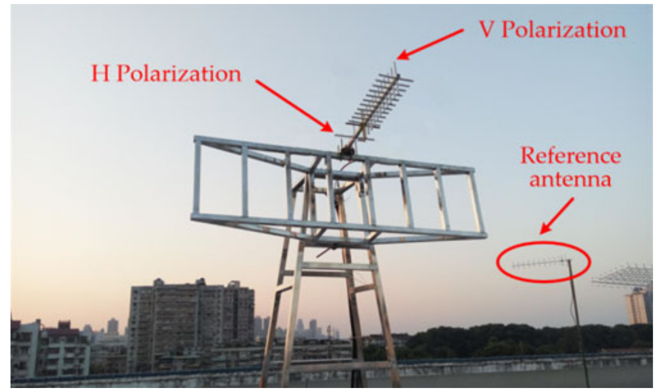

Fig. 4. Antenna system.

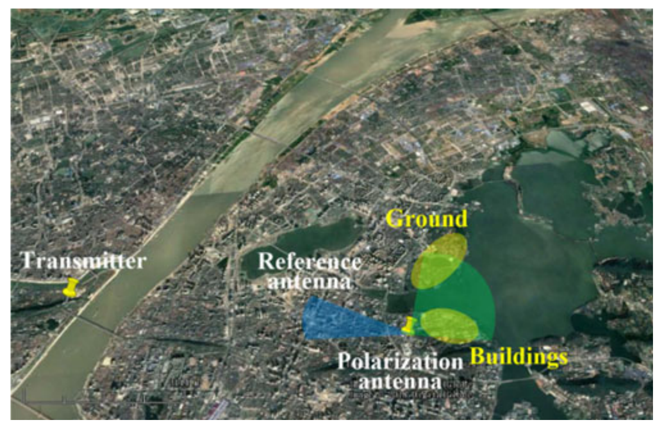

Fig. 5. Experimental geometry.

Experimental setup

The experimental system consists of reference antenna, surveillance antenna, multi-channel receiver, and upper computer. The surveillance antenna [33] is shown in Fig. 4. The whole antenna system is composed of one pair of dual-polarization antenna and one pair of single polarization antenna. Dual-polarization antenna is called surveillance antenna and used to receive surveillance signal. Single polarization antenna is used to receive reference signal and called reference antenna. The polarization isolation of surveillance antenna in the frequency band (710–718 MHz) is >20 dB. The gain of surveillance antenna is ∼10 dB.

As shown in Fig. 5, the green sector area represents surveillance antenna beam direction. The blue sector area represents reference antenna beam direction. The yellow elliptical area represents ground and buildings which bring clutter. The detection target was Boeing 737 plane.

Experimental analysis

The SDPPR system needs to reconstruct the reference signal from the surveillance channel. In order to verify the effectiveness of the method proposed in this paper, the surveillance antenna of the SDPPR system was pointed at an angle of 120° with the transmitter, so as to weaken the influence of direct-path signal on the surveillance signal. In this scenario, we can obtain the surveillance signal spectrum as shown in Fig. 6(a), and the constellation

https://doi.org/10.1017/S1759078722001222 Published online by Cambridge University Press

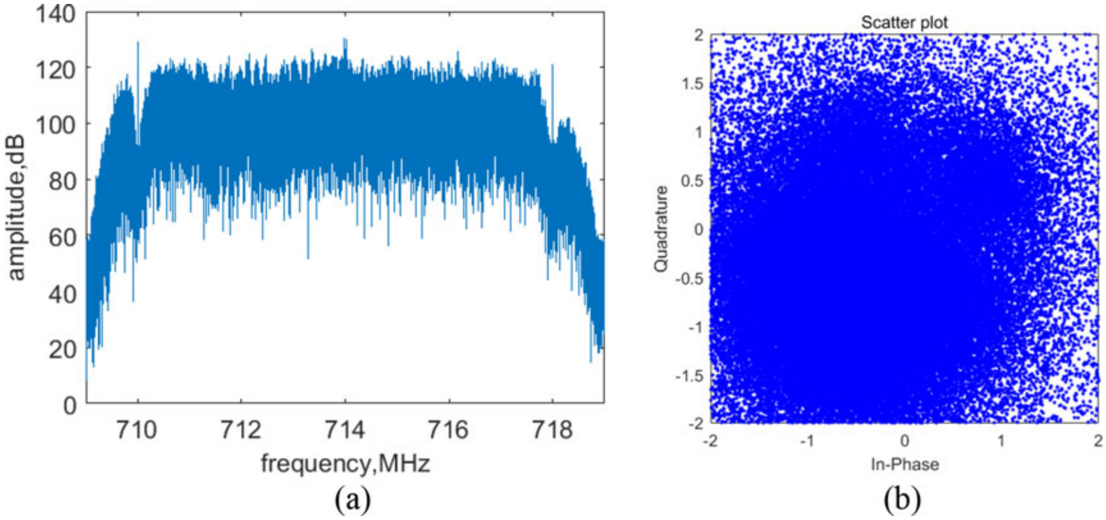

Fig. 6. Surveillance channel data: (a) signal frequency spectrum and (b) constellation diagram.

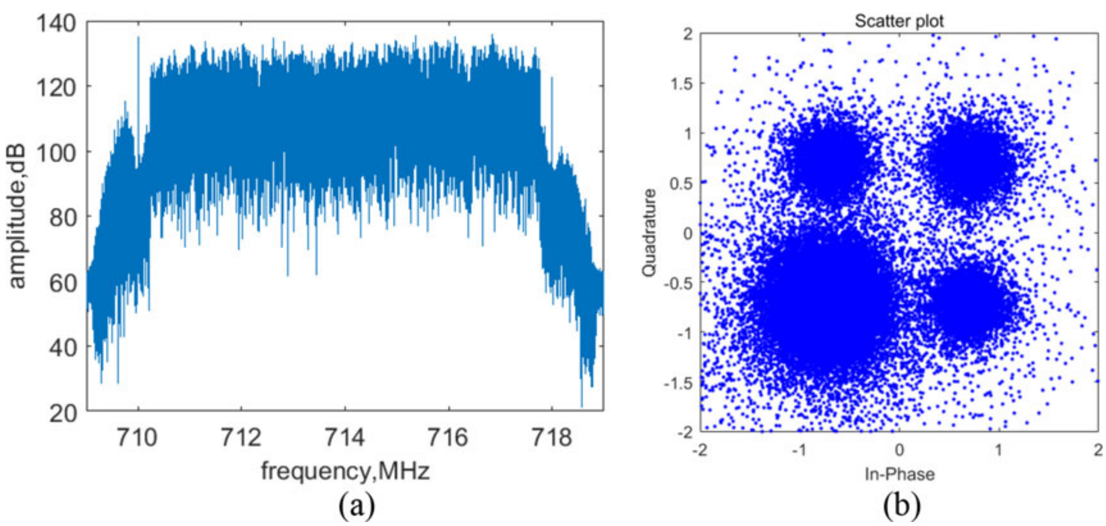

Fig. 7. Reference channel data: (a) signal frequency spectrum and (b) constellation diagram.

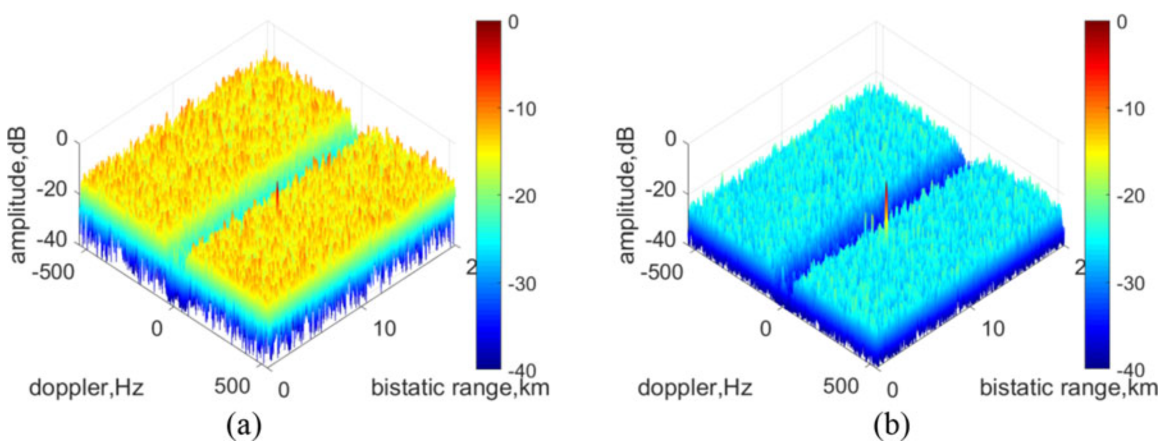

Fig. 8. RD maps in the 80-th frame in RSR: (a) RD map of *V* channel and (b) RD map of *H* channel.

https://doi.org/10.1017/S1759078722001222 Published online by Cambridge University Press

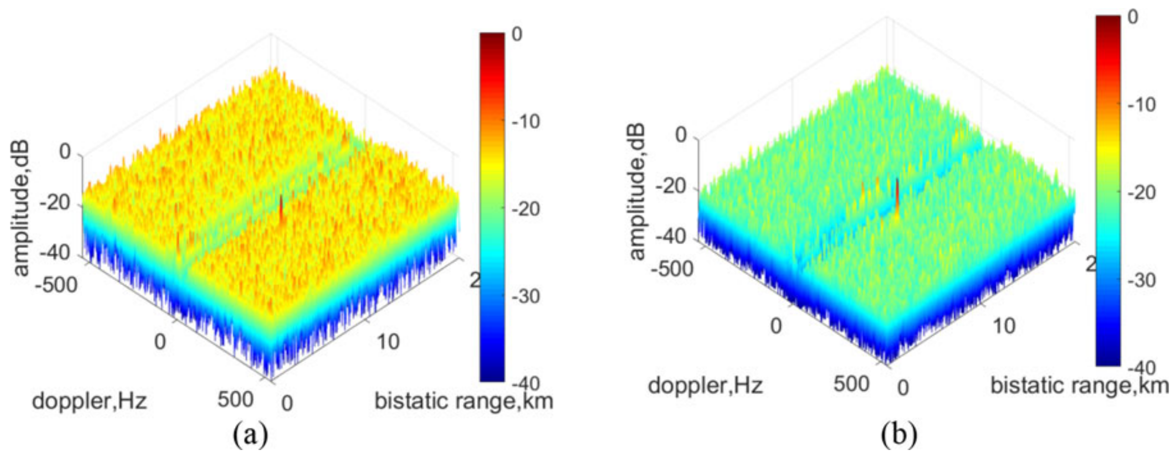

Fig. 9. RD maps in the 80-th frame in RSMP: (a) RD map in *V* channel and (b) RD map in *H* channel.

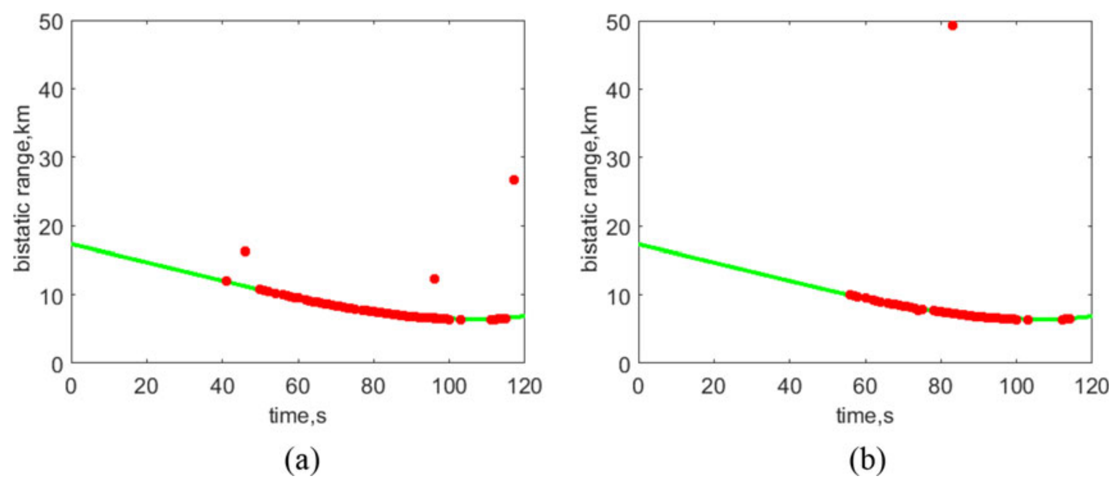

Fig. 10. Result of target detection: (a) detection result in RSR and (b) detection result in RSMP.

diagram on surveillance signal as shown in Fig. 6(b). When using the reference antenna to collect data, the received signal spectrum is shown in Fig. 7(a), and the signal constellation diagram is shown in Fig. 7(b).

In the effective bandwidth, the signal spectrum amplitude of the reference channel is at least 10 dB stronger than that of the surveillance channel, which also means that the SNR of the direct-path signal in the reference channel is much stronger than that in the surveillance channel. Therefore, the reference channel signal constellation is more focused than the surveillance channel constellation. In this scenario, the reference signal cannot be reconstructed from the surveillance channel.

The experimental data were collected from a Boeing 737 in the radar surveillance area. After obtaining the reference signal, we perform time-domain filtering and matched filtering on the *V*-polarized channel and *H*-polarized channel data, respectively. When the reference signal is obtained from the reference channel using signal reconstruction, the range Doppler (RD) map of the *H*-polarized channel and the *V*-polarized channel are shown in Fig. 8. When using the method in this paper to obtain the reference signal from the surveillance channel, the RD map of the *H*-polarized channel and the *V*-polarized channel are shown in Fig. 9.

It can be seen from Figs 8 and 9, whether it is the *H*-polarized channel or the *V*-polarized channel, the reference signal obtained based on the reconstruction method has a better clutter suppression effect. This is because the SNR of the reference signal extracted from the surveillance channel is lower than that obtained from the reference channel reconstruction. However, the target peak is still evident in Fig. 9.

The RD map data of the *H*-polarized and *V*-polarized channels were fused [34], and then the cell-average constant false alarm rate detection was performed, and the detection results are shown in Fig. 10. The red dots represent the target detection points. The green line represents the target real track obtained from the automatic-dependent surveillance broadcast system.

The detection result by using the RSR method as shown in Fig. 10 (a). The target detection points are very continuous between the 50th and 100th seconds. The detection result by using the RSMP method as shown in Fig. 10(b). Although the reference signal cannot be reconstructed from the surveillance channel, the detection points obtained by using the RSMP method are still satisfactory.

https://doi.org/10.1017/S1759078722001222 Published online by Cambridge University Press

Table 2. Target detection statistical result

Method	Data length (frames)	Detection points	Detection rate (%)
RSR-RC	120	52	43.3
RSR-SC		Fail	Fail
RSMP-SC		44	36.7

In the scenario set in this paper, the statistics of the target detection results are shown in Table 2.

In Table 2, we can clearly see that the best result is obtained by using the reference signal reconstruction from reference channel (RSR-RC) method, followed by the reference signal extraction in multi-processing from surveillance channel (RSMP-SC) method. The reference signal reconstruction from surveillance channel (RSR-SC) method cannot obtain reference signal, and the target detection fails. For the SDPPR system, there are only one surveillance antenna and no reference antenna, so the conventional method to obtain reference signal is signal reconstruction. However, in urban environments, due to factors such as terrain and interference, signal reconstruction may fail. The method proposed in this paper can solve the above problems and is an effective alternative.

Conclusion

In this paper, a combined reference signal extraction method of SDPPR system based on sub-carrier processing, blind adaptive oblique projection technology and ECA is studied. This method is different from the signal reconstruction method. When the SNR of the direct-path signal is low and the reference signal cannot be reconstructed, the reference signal can still be extracted in the RSMP method. This can greatly improve the adaptability of the SDPPR system in complex urban environment scenarios. Therefore, the RSMP method can be used as an effective supplement to the RSR method.

Acknowledgements. The authors acknowledge Wuhan University for supporting the work of this paper. This work was supported by the National Nature Science Foundation of China (61967007, 61963016), the Key Research and Development Program of Jiangxi Province (20202BBEL53014, 20201BBF61012), Natural Science Foundation of Jiangxi Province (20212BAB202005), the Research Project of National Defence Science and Technology Key Laboratory Foundation (6142113180101), and the Jiangxi Province Department of Education Science and Technology Research Key Project (GJJ200667, GJJ170360).

Conflict of interest. The authors report no conflict of interest.

References

1. **Colone F, O'Hagan DW, Lombardo P and Baker CJ** (2009) A multistage processing algorithm for disturbance removal and target detection in passive bistatic radar. *IEEE Transactions on Aerospace and Electronic Systems* **45**, 698–722.
2. **Wan XR, Yi JX, Zhao ZX and Ke HY** (2014) Experimental research for CMMB-based passive radar under a multipath environment. *IEEE Transactions on Aerospace and Electronic Systems* **50**, 70–85.
3. **Malanowski M, Kulpa K and Misiurewicz J** (2008) PaRaDe: passive radar demonstrator family development at Warsaw University of Technology. *IEEE Microwaves Radar and Remote Sensing Symposium, Kiev, Ukraine, 22–24 September*, pp. 75–78.
4. **Poullin D** (2005) Passive detection using digital broadcasters (DAB, DVB) with COFDM modulation. *IEE Proceedings on Radar Sonar and Navigation* **152**, 143–152.
5. **Coleman C and Yardley H** (2008) Passive bistatic radar based on target illuminations by digital audio broadcasting. *IET Proceedings on Radar Sonar and Navigation* **2**, 366–375.
6. **Colone F, Woodbridge K, Guo H, Mason D and Baker CJ** (2011) Ambiguity function analysis of wireless LAN transmissions for passive radar. *IEEE Transactions on Aerospace and Electronic Systems* **47**, 240–264.
7. **Tan DKP, Sun H, Lu Y, Lesturgle M and Chan HL** (2005) Passive radar using global system for mobile communication signal: theory, implementation and measurements. *IEE Proceedings on Radar Sonar and Navigation* **152**, 116–123.
8. **Bartoletti S, Conti A and Win MZ** (2014) Passive radar via LTE signal of opportunity. *IEEE International Conference on Communications Workshops, Sydney, NSW, Australia, 10–14 June*, pp. 1–5.
9. **Zhao JH, Ni S, Yang L, Zhang Z, Gong Y and Yu X** (2019) Multiband cooperation for 5G HetNets: a promising network paradigm. *IEEE Vehicular Technology Magazine* **14**, 85–93.
10. **Zhao JH, Liu J, Yang L, Ai B and Ni S** (2021) Future 5G-oriented system for urban rail transit: opportunities and challenges. *China Communication* **18**, 1–12.
11. **Colone F, Cardinali R, Lombardo P, Crognale O, Cosmi A, Lauri A and Bucciarelli T** (2009) Space-time constant modulus algorithm for multipath removal on the reference signal exploited by passive bistatic radar. *IET Radar Sonar and Navigation* **3**, 253–264.
12. **Palmer JE, Harms HA, Searle SJ and Davis LM** (2013) DVB-T passive radar signal processing. *IEEE Transactions on Signal Processing* **61**, 2116–2126.
13. **Baczyk MK and Malanowski M** (2010) Decoding and reconstruction of reference DVB-T signal in passive radar systems. *IEEE International Radar Symposium (IRS). Vilnius, Lithuania, 16–18 June*, pp. 1–4.
14. **O'Hagan DW, Kuschel H, Heckenbach J, Ummenhofer M and Schell J** (2010) Signal reconstruction as an effective means of detecting targets in a DAB-based PBR. *IEEE International Radar Symposium (IRS). Vilnius, Lithuania, 16–18 June*, pp. 1–4.
15. **Zemmari R** (2010) Reference signal extraction for GSM passive coherent location. *IEEE International Radar Symposium (IRS). Vilnius, Lithuania, 16–18 June*, pp. 1–4.
16. **Wan XR, Wang JF, Hong S and Tang H** (2011) Reconstruction of reference signal for DTMB-based passive radar systems. *IEEE CIE International Conference on Radar. Chengdu, China, 24–27 October*, pp. 165–168.
17. **Searle S, Davis L and Palmer J** (2015) Signal processing considerations for passive radar with a single receiver. *IEEE International Conference on Acoustics, Brisbane, Australia, 19–24 April*, pp. 5560–5564.
18. **Yi YC, Wan XR, Yi JX and Cao XM** (2019)Polarization diversity technology research in passive radar based on subcarrier processing. *IEEE Sensors Journal* **19**, 1710–1719.
19. **Yi YC, Wan XR, Yi JX and Cao XM** (2018) Polarization experimental research of passive radar based on digital television signal. *Electronics Letters* **54**, 385–387.
20. **Behrens RT and Scharf LL** (1994) Signal processing applications of oblique projection operators. *IEEE Transactions on Signal Processing* **42**, 1413–1424.
21. **Boyer R and Bouleux G** (2008) Oblique projections for direction of arrival estimation with prior knowledge. *IEEE Transactions on Signal Processing* **56**, 1374–1387.
22. **Mao XP, Liu AJ, Hou HJ, Hong H, Guo R and Deng WB** (2012) Oblique projection polarisation filtering for interference suppression in high-frequency surface wave radar. *IET Radar Sonar and Navigation* **6**, 71–80.

23. **Mccloud ML and Scharf LL** (2002) A new subspace identification algorithm for high-resolution DOA estimation. *IEEE Transactions on Antennas and Propagation* **50**, 1382–1390.
24. **Cao B, Zhang QY, Liang D, Wen SM, Jin L and Zhang YQ** (2010) Blind adaptive polarization filtering based on oblique projection. *IEEE International Conference on Communications, Cape Town, South Africa, 23–27 May*, pp. 1–5.
25. **Hou HJ, Mao XP and Li SB** (2012) A generalized oblique projection operator for interference suppression under colored noise. *IEEE Radar Conference, Atlanta, USA, 7–11 May*, pp. 687–692.
26. **Yi CL, Ji ZY, Kirubarajan T, Xie JH and Hu B** (2016) An improved oblique projection method for sea clutter suppression in shipborne HFSWR. *IEEE Geoscience and Remote Sensing Letters* **13**, 1089–1093.
27. **Tannaka A and Imai H** (2014) Music-based DOA estimation by oblique projection along the signal subspace. *IEEE Workshop on Statistical Signal Processing, Gold Coast, Australia, 2 July–29 June*, pp. 300–303.
28. **Sun ML, Xie JH, Hao ZW and Yi CL** (2012) Target detection and estimation for shipborne HFSWR based on oblique projection. *IEEE International Conference on Signal Processing, Beijing, China, 21–25 October*, pp. 386–389.
29. **Wang J, Zhang QY and Cao B** (2009) Multi-notch polarization filtering based on oblique projection. *IEEE Global Mobile Congress, Shanghai, China, 12–14 October*, pp. 1–6.
30. **Coon J, Sandell M, Beach M and Mcgeehan J** (2006) Channel and noise variance estimation and tracking algorithms for unique-word based single-carrier systems. *IEEE Transactions on Wireless Communication* **5**, 1488–1496.
31. **Boumard S** (2003) Novel noise variance and SNR estimation algorithm for wireless MIMO OFDM systems. *IEEE Global Telecommunication Conference, San Francisco, USA, 1–5 December*, pp. 1330–1334.
32. **Yi JX, Wan XR, Li DS and Leung H** (2018) Robust clutter rejection in passive radar via generalized subband cancellation. *IEEE Transactions on Aerospace and Electronic Systems* **54**, 1931–1946.
33. **Cao XM, Gong ZP, Yi YC, Wang BJ and Wan XR** (2016) Design of a dual-polarized Yagi-Uda antenna for the passive radar. *IEEE Conference Publications. Guilin, China, 18–21 October*, pp. 125–128.
34. **Yi YC, Zhu L and Cao XM** (2022) Signal fusion research in passive radar based on polarization diversity technology. *International Journal of Microwave and Wireless Technologies*, 1–14.

Yucheng Yi was born in Hunan, China, in 1985. He received his Ph.D. degree from the School of Electronic Information, Wuhan University. He is now a lecturer in the School of Information Engineering, East China Jiaotong University. His main research interests include radar signal processing and polarization array signal processing.

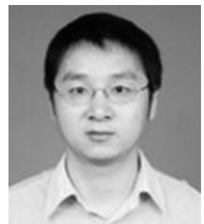

Lu Zhu was born in Jiangxi, China, in 1976. He received his Ph.D. degree from the Huazhong University of Science and Technology. He is now a professor and master supervisor in the School of Information Engineering, East China Jiaotong University. Recently, he has hosted and participated in more than 10 national research projects.

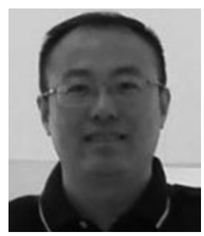

Long Liang was born in Shandong, China, in 1985. He received his Ph.D. degree from the School of Electronic Information, Wuhan University. His main research interests focus on airborne passive radar.

Yan Fu was born in Hubei, China, in 1989. He received his Ph.D. degree from the School of Electronic Information, Wuhan University. His main research interests include interference suppression, radar detection, and FM radar.

https://doi.org/10.1017/S1759078722001222 Published online by Cambridge University Press